Noise-induced transitions in coupled oscillator systems with a pinning force

Seunghwan Kim,* Seon Hee Park, and Chang Su Ryu
Research Department, Electronics and Telecommunications Research Institute, P.O. Box 106, Yusong-gu, Taejon, 305-600, Korea
(Received 23 July 1996)

We investigate noise-induced transitions in coupled oscillator systems with higher harmonic pinning force subject to a fluctuating interaction and a thermal additive noise. It is shown that the thermal additive noise induces a symmetry-breaking transition at a critial thermal noise intensity that does not depend on the strength of the fluctuating interaction. The critical line is found analytically in the parameter space of the pinning force and thermal noise intensity. The fluctuating interaction brings about bifurcations of a stationary probability distribution leading to the clustering of oscillators at its critical strengths, which depend on the thermal noise intensity and the strength of the pinning force. The cooperation of the thermal noise, the fluctuating interaction, and the pinning force provides the rich structure of phase diagrams such as a reentrant transition. The nature of the transitions is also discussed in detail. [S1063-651X(96)01112-9]

PACS number(s): 02.50.Ey, 05.70.Fh

I. INTRODUCTION

The effect of noise on a dynamical system has been studied extensively in the context of equilibrium and nonequilibrium phenomena. The study of phase transitions, originally limited to equilibrium systems, was extended to nonequilibrium systems [1]. While a thermal additive noise provides equilibrium phenomena such as a disordering effect and a symmetry-breaking transition, a multiplicative noise coupled to the state of the system induces nonequilibrium phenomena such as a change of the stability of the system. In some cases, new stable states appear under the influence of strong multiplicative noise. One may find examples in models of biology [2], chemical reactions [3], optics [4], plasma physics [5], etc., which have phenomenological justifications [6]. Transitions induced by the multiplicative noise in low-dimensional dynamical systems are by now a familiar phenomena [1], but the multiplicative noise in spatially distributed and/or high-dimensional systems remains the focus of current research [7]. The question of the interplay between multiplicative and additive noises in the systems has been raised continuously [8].

Coupled phase oscillators have been studied extensively as a model system to understand the dynamics of a variety of systems ranging from Josephson-junction arrays [9] to chemical reactions [10] to charge-density waves [11]. In neuronal signal processing, the synchronous oscillations found in the visual cortex have been modeled and understood via coupled phase oscillators [12]. Recently, the system with a pinning force has been provided as a model system to study the interplay between the multiplicative and additive noises in the spatially distributed system [13,14]. In the system the additive noise induces a transition from a moving state to a stationary state and the multiplicative noise induces a transition from a one-cluster state to a two-cluster state both in stationary and moving phases showing a route to the clustering phenomenon. It has also been shown that there is a reentrant transition induced by the interplay of the multiplicative and additive noises.

In this paper we study extensively the nonequilibrium phenomena of the globally coupled oscillator systems with a higher harmonic pinning force subject to a fluctuating interaction and a thermal additive noise. It is shown that the thermal additive noise induces a symmetry-breaking transition at a critical thermal additive noise intensity that does not depend on the strength of the fluctuating interaction. The critical line is found analytically in the parameter space of the pinning force and thermal noise intensity. The fluctuating interaction brings about noise-induced transitions forming clusters at its critical strengths, which depend on the thermal noise intensity and the strength of the pinning force. The cooperation of the thermal noise, the fluctuating interaction, and the pinning force provides the rich structure of phase portraits such as a reentrant transition. The nature of the transitions is also discussed in detail.

In the following section we describe the coupled oscillator model with a higher harmonic pinning force. In Sec. III we derive a formal solution of the Fokker-Planck equation. In Sec. IV the interplay between the nonequilibrium transitions due to the multiplicative noise and the symmetry-breaking transition due to the thermal noise are studied in detail. The noise-induced transition and the symmetry-breaking transition of the system are studied in Sec. IV, showing the rich structure of the phase portraits. The nature of the phase transitions is also discussed with summarized results in Sec. V.

II. MODEL

A (noiseless) model of N coupled oscillators with a μth harmonic pinning force under study is expressed by the equation of motion

$$\frac{d\phi_i}{dt} = \omega_i - b_i \sin(\mu\phi_i) - \sum_{j=1}^{N} K_{ij} \sin(\phi_i - \phi_j) \ , \qquad (1)$$

where ϕ_i and ω_i, $i=1,2,\ldots,N$, are the phase and the intrinsic frequency of the ith oscillator, respectively. On the right-hand side of Eq. (1) the second term is a μth harmonic

*Electronic address: skim@logos.etri.re.kr

pinning force and the third term describes global coupling that depends on the phase difference of two oscillators. In the absence of the pinning force the system has been studied extensively in the context of entrainment of population and synchronization of oscillators. The pinning force has been introduced to mimic the dynamics of stochastic limit cycle oscillators or excitable elements [15].

In the uniform frequency $\omega_i=\omega$, if the coupling is excitatory, i.e., $K_{ij}>0$, then the global coupling gives perfect synchrony, which means $\phi_i(t)=\phi(t)$ for all i. The steady state of Eq. (1) is the ground state of the system with the Hamiltonian

$$H=\sum_i \left(\omega_i\phi_i-\frac{b}{\mu}\cos(\mu\phi_i)\right)-\sum_{(ij)} K_{ij}\cos(\phi_i-\phi_j) \ , \qquad (2)$$

where the (ij) summation is taken over all pairs (each pair counted only once). For the case of uniform frequency and excitatory coupling, every ϕ_i dwells on one of the $\mu+1$ phases. When $|b/\omega|>1$, the Hamiltonian Eq. (2) has μ local minima at

$$\phi_i=\phi_n\equiv\frac{1}{\mu}\sin^{-1}\left(\frac{\omega}{b}\right)+\frac{2\pi n}{\mu} \ , \quad n=0,1, \ldots ,\mu-1, \quad (3)$$

and all elements are at the same stable fixed point ϕ_n. When $|b/\omega|<1$, Eq. (2) has no local minimum, implying that the system is in the moving phase, i.e., each ϕ_i is a rotator with frequency $\sqrt{\omega^2-b^2}$. The pinning force of Eq. (1) generates the μ stationary states and characterizes the system whether it is in the stationary state or the moving state.

Now we assume the uniform frequency and excitatory interaction, i.e., $\omega_i=\omega$ and $K_{ij}=K/N>0$. If the system is coupled to a fluctuating environment, the coupling strength then may be assumed to be a stochastic quantity, which implies

$$\frac{K}{N}\rightarrow\frac{1}{N}[K+\sigma_M\eta_i(t)] \ , \qquad (4)$$

where $\eta_i(t)$ is a Gaussian white noise characterized by

$$\langle\eta_i(t)\rangle=0 \ , \quad \langle\eta_i(t)\,\eta_j(t')\rangle=2\delta_{ij}\delta(t-t') \qquad (5)$$

and σ_M measures the strength of the fluctuating interaction. This multiplicative noise has been introduced to provide a route to clustering phenomena without introducing higher Fourier mode interactions [13]. It has been shown in Ref. [13] that in the presence of the multiplicative noise the system shows a bifurcation from a one-cluster state to a multicluster state in both stationary and moving phases, which cannot be seen in the deterministic case or in the system with a simple additive noise.

For small multiplicative noise intensity the perfect synchrony of the system persists, leading to the singularity of the probability distribution of the Fokker-Planck equation corresponding to the equation of motion of the system [14]. To remove the singularity we introduce an additive noise $\xi_i(t)$ to the system. The interplay between the additive and multiplicative noises also induces interesting nonequilibrium phenomena such as a reentrant transition [14]. Thus, in the presence of the additive noise as well as the multiplicative noise, Eq. (1) is replaced by the stochastic differential equation

$$\frac{d\phi_i}{dt}=\omega-b\sin(\mu\phi_i)-\frac{1}{N}[K+\sigma_M\eta_i(t)]\sum_{j=1}^{N}\sin(\phi_i-\phi_j) + \sigma_A\xi_i(t) \ , \qquad (6)$$

where $\xi_i(t)$ is a Gaussian white noise independent of $\eta_i(t)$'s. $\xi_i(t)$ is characterized by

$$\langle\xi_i(t)\rangle=0 \ , \quad \langle\xi_i(t)\xi_j(t')\rangle=2\delta_{ij}\delta(t-t') \ , \qquad (7)$$

$$\langle\xi_i(t)\,\eta_j(t')\rangle=0 \qquad (8)$$

and σ_A measures the intensity of the additive noise. Throughout this paper we set $K=1$ using a suitable time unit.

Equation (6) is invariant under the global finite translations

$$\phi_i\rightarrow\phi_i+\frac{2\pi n}{\mu} \ , \quad n=1,2, \ldots ,\mu-1, \qquad (9)$$

for all ϕ_i's. When $\omega=0$ Eq. (6) is also invariant under the global inversion

$$\phi_i\rightarrow-\phi_i \qquad (10)$$

for all ϕ_i's. Numerical simulations for $\mu=1$, 2, and 3 with $\omega=0$ show that the global inversion symmetry persists regardless of the additive and multiplicative noise intensities. However, the global finite translation symmetry is broken at small additive noise intensity, which is shown in the following section.

III. FORMAL SOLUTION OF THE FOKKER-PLANCK EQUATION

The macroscopic behavior of the system can be described by the probability distribution $P(\phi,t)$ of ϕ_i at time t, whose evolution is governed by the Fokker-Planck equation [16]. In the large-N limit, the stochastic differential equation (6) yields the Fokker-Planck equation

$$\frac{\partial P}{\partial t}=-\frac{\partial}{\partial\phi}\left[\left\{\omega-b\sin(\mu\phi)-\int_0^{2\pi}d\phi'\sin(\phi-\phi')n(\phi',t) + \nu\sigma_M^2\int_0^{2\pi}d\phi'\sin(\phi-\phi')n(\phi',t) \times\int_0^{2\pi}d\phi''\cos(\phi-\phi'')n(\phi'',t)\right\}P(\phi,t)\right] + \frac{\partial^2}{\partial\phi^2}\left[\left\{\sigma_A^2+\sigma_M^2\left(\int_0^{2\pi}d\phi'\sin(\phi-\phi')n(\phi',t)\right)^2\right\} \times P(\phi,t)\right] \ , \qquad (11)$$

with $\nu=1$ for the Stratonovich interpretation and $\nu=0$ for Itô interpretation [17]. In Eq. (11) $n(\phi,t)$, the normalized

number density of the oscillators with phase ϕ at time t, is given by

$$n(\phi,t)=\frac{1}{N}\sum_{i=1}^{N}\delta(\phi_i(t)-\phi)\ . \tag{12}$$

Since the ϕ_i's are statistically independent for the uniform interaction, $n(\phi,t)$ may be identified with $P(\phi,t)$. In this paper we will analyze the steady-state probability distribution $P(\phi)$ achieved as $t\to\infty$.

Assuming the stationary state, i.e., $\partial P/\partial t=0$, the steady state of Eq. (11) is given by

$$P(\phi)=\exp\left[\int_0^{\phi}f(\phi')d\phi'\right]\left\{P(0)-J\int_0^{\phi}d\phi'\times\exp\left[-\int_0^{\phi'}f(\phi'')d\phi''\right]g(\phi')\right\}\ , \tag{13}$$

where

$$f(\phi)=\frac{[\omega-b\sin(\mu\phi)-\Delta\sin(\phi-\alpha)-(2-\nu)\sigma_M^2\Delta^2\sin(\phi-\alpha)\cos(\phi-\alpha)]}{[\sigma_A^2+\sigma_M^2\Delta^2\sin^2(\phi-\alpha)]}\ , \tag{14}$$

$$g(\phi)=\frac{1}{\sigma_A^2+\sigma_M^2\Delta^2\sin^2(\phi-\alpha)} \tag{15}$$

with $\Delta=\sqrt{C^2+S^2}$ and $\alpha=\sin^{-1}(S/C)$. Here C and S are obtained by the self-consistent equations

$$C=\int_0^{2\pi}\cos\phi P(\phi)d\phi\ ,\quad S=\int_0^{2\pi}\sin\phi P(\phi)d\phi\ . \tag{16}$$

In Eq. (13), J is the constant probability current that is imposed by the boundary condition

$$P(\phi+2\pi)=P(\phi)\ . \tag{17}$$

When $\omega=0$, since the Fokker-Planck equation (11) is invariant under the global inversion (10) we can assume $P(\phi)$ to be an even function, i.e., $P(-\phi)=P(\phi)$. This symmetry is confirmed for small μ, i.e., $\mu=1$, 2, and 3, by extensive numerical simulations leading to $S=0$. Since $\int_0^{2\pi}f(\phi)=0$ with $S=0$ the boundary condition (17) results in $J=0$. Then the stationary probability distribution is written as

$$P(\phi)=\frac{1}{Z}\exp\left[\int_0^{\phi}f(\phi')d\phi'\right]\ , \tag{18}$$

where

$$f(\phi)=\frac{-b\sin(\mu\phi)-\Delta\sin\phi[1+(2-\nu)\sigma_M^2\Delta\cos\phi]}{\sigma_A^2+\sigma_M^2\Delta^2\sin^2\phi}\ ,$$

$$Z=\int_0^{2\pi}\exp\left[\int_0^{\phi}f(\phi')d\phi'\right]d\phi\ , \tag{19}$$

with the self-consistent equation

$$\Delta=\int_0^{2\pi}\cos\phi P(\phi)d\phi\ . \tag{20}$$

In Eq. (18), if and only if $\Delta=0$, $P(\phi)$ has the translational symmetries (9) and thus nonzero Δ means that the translational symmetries are broken. Thus Δ plays the role of an order parameter for the symmetries. For small Δ expanding $P(\phi)$ as a power series of Δ, we obtain the self-consistent equation (20) as

$$\Delta=A_\mu^{(0)}+A_\mu^{(1)}\Delta+A_\mu^{(2)}\Delta^2+A_\mu^{(3)}\Delta^3+O(\Delta^4)\ , \tag{21}$$

where

$$A_\mu^{(0)}=\frac{C_1\left(\frac{b}{\sigma_A^2}\right)}{C_0\left(\frac{b}{\sigma_A^2}\right)}\delta_{\mu,1},$$

$$A_\mu^{(1)}=\frac{1}{2\sigma_A^2}\left[1+\left\{\frac{C_2\left(\frac{b}{\sigma_A^2}\right)}{C_0\left(\frac{b}{\sigma_A^2}\right)}-2\right\}\delta_{\mu,1}+\frac{C_1\left(\frac{b}{2\sigma_A^2}\right)}{C_0\left(\frac{b}{2\sigma_A^2}\right)}\delta_{\mu,2}\right], \tag{22}$$

$$A_\mu^{(2)}=A_1^{(2)}\delta_{\mu,1}+A_3^{(2)}\delta_{\mu,3},$$

with

$$C_\mu(x)\equiv\int_0^{2\pi}\cos(\mu\phi)\exp[x\cos\phi]d\phi\ . \tag{23}$$

In Eqs. (21) and (22), $A_1^{(2)}$, $A_3^{(2)}$, and $A_\mu^{(3)}$ are very complicated functions of σ_A, σ_M, and b. When $\mu=1$ nonzero $A_1^{(0)}$ provides finite Δ for all parameter values, implying that the system with $\mu=1$ has no translational symmetry. Thus, for $\mu=1$ there is no symmetry-breaking transition at finite parameter values.

For $\mu>1$, $A_\mu^{(0)}=0$ means that, assuming a continuous transition, there is a symmetry-breaking transition at $A_\mu^{(1)}=1$: For $A_\mu^{(1)}>1$, $\Delta>0$, implying a symmetry-breaking phase, and for $A_\mu^{(1)}<1$, $\Delta=0$, implying a symmetric phase. When $\mu=2$, the critical line $A_2^{(1)}=1$ is given by

$$\sigma_{Ac}=\sqrt{\frac{1}{2}\left(1+\frac{C_1(x)}{C_0(x)}\right)}\ , \quad b=x\sigma_{Ac}\,, \tag{24}$$

with $x\in(0,\infty)$ for all σ_M. The solid line in Fig. 4(b) separating asymmetric one-cluster (S_s) and two-cluster (S_d) phases from a symmetric (D) phase shows the critical line, which is independent of σ_M. When $\mu>2$, the critical point is given by $\sigma_{Ac}=1/\sqrt{2}$ for all σ_M and b. Since $A_\mu^{(2)}$ is nonzero only for $\mu=1$ and 3, the scaling exponent, defined by

$$\Delta\sim(A_\mu^{(1)}-1)^\beta \tag{25}$$

when $A_\mu^{(1)}$ approaches to 1 from above, is given by

$$\beta=\begin{cases}1 & \text{for } \mu=3\\ \frac{1}{2} & \text{for } \mu=2, \quad \mu>3.\end{cases} \tag{26}$$

The critical lines and the scaling exponents do not depend on the multiplicative noise intensity. The multiplicative noise only changes the mulitplicative factor of the scaling equation (25). Since the interaction between oscillators in Eq. (6) depends on the phase difference of two oscillators, the multiplicative noise coupled to the interaction does not restore the translational symmetry broken by the pinning force, implying that σ_{Ac} is independent of σ_M.

The noise-induced transitions are characterized by the change of the number of peaks in the stationary probability distribution $P(\phi)$. $P(\phi)$ has extrema at zeros of $f(\phi)$ given by Eq. (19). Using the identity

$$\sin(\mu\phi)=\sin\phi\sum_{k=0}^{\mu-1}\cos^k\phi\cos[(\mu-1-k)\phi]\ , \tag{27}$$

the zeros of $f(\phi)$ are given by the roots of

$$\sin\phi\left[b\sum_{k=0}^{\mu-1}\cos^k\phi\cos[(\mu-1-k)\phi]+\Delta+(2-\nu)\sigma_M^2\Delta^2\cos\phi\right]=0\,. \tag{28}$$

When $b=\sigma_M=0$, Eq. (28) has zeros at $\phi=0$ and π, leading to $P(\phi)$, which has a peak at $\phi=0$. As b and σ_M increase the number of roots of Eq. (28) and thus the number of peaks of $P(\phi)$ increase at critical values of b and σ_M, leading to the noise-induced transition. We identify multiple peaks in the distribution as corresponding to multiple clusters of like-phased oscillators. That is, we interpret the distribution as the instantaneous distribution of oscillator phases rather than as the distribution over time of the average phase. These are two physically distinct interpretations; which one is correct can be (and was) checked in actual direct simulations of the globally coupled system. We found that the cluster interpretation is valid. We present the phase diagrams for $\mu=1$, 2, and 3 in the following section.

IV. PHASE TRANSITIONS

A. $\mu=1$

When $\mu=1$, it has been shown in Sec. III that there is no symmetry-breaking transition due to the additive thermal noise. Performing the integration in Eq. (18) with $\mu=1$ we obtain

$$P(\phi)=Z^{-1}(1+A\cos\phi)^{\gamma-(2-\nu)/2}(1-A\cos\phi)^{-\gamma-(2-\nu)/2}\ , \tag{29}$$

where

$$\gamma=\frac{b+\Delta}{2\sigma_M\Delta\sqrt{\sigma_A^2+\sigma_M^2\Delta^2}}, \quad A=\frac{\sigma_M\Delta}{\sqrt{\sigma_A^2+\sigma_M^2\Delta^2}} \tag{30}$$

with a self-consistent equation (20). For given values of γ and A, Δ can be obtained from Eq. (20) together with Eq. (29) and σ_A, σ_M, and b are related by

$$\sigma_M=\frac{A}{\Delta(A,\gamma)\sqrt{1-A^2}}\sigma_A\,, \quad b=\frac{2A\gamma}{1-A^2}\sigma_A^2-\Delta(A,\gamma)\ . \tag{31}$$

For all sets of σ_M, σ_A, and b satisfying Eq. (31), $P(\phi)$ is given by Eq. (29). $P(\phi)$ has a maximum at $\phi=0$ or 2π. With a definition of $\Gamma\equiv 2\gamma/(2-\nu)A$, Eq. (29) shows that for $\Gamma>1$, $P(\phi)$ has a minimum at $\phi=\pi$, and for $\Gamma<1$, $P(\phi)$ has a local maximum at $\phi=\pi$ and a minimum at $\phi=\cos^{-1}(-\Gamma)$. The critical point where a bifurcation $S_s\rightarrow S_d$ occurs is given by Eq. (31) with $\gamma=(2-\nu)A/2$ for $A\in[0,1]$.

In Fig. 1 we show the phase portraits in the Stratonovich interpretation with $\nu=1$. In the Itô interpretation with $\nu=0$, the phase portraits show a similar structure to those in the Stratonovich interpretation [14]. Figure 1(a) shows the phase diagrams in the σ_M-σ_A plane for various values of b. For a given σ_A, an S_s state exists at small σ_M. An S_d state appears at a critical value of σ_M, σ_{Mc}, at which the transition induced by the multiplicative noise occurs. The phase realization of the system is affected by the additive noise intensity for fixed $\sigma_M>\sigma_{Mc}$, which is not the case when the system has only additive noise. σ_{Mc} increases as σ_A increases, implying that the additive noise suppresses the effect of the multiplicative noise, which tends to split the oscillators into clusters. In the limit $\sigma_A\rightarrow\infty$, $\sigma_{Mc}=2\sigma_A/\sqrt{b(2-\nu)}$. As σ_A goes to zero, σ_{Mc} approaches to $\sqrt{(b+1)/(2-\nu)}$. When $b=0$, in the limit $\sigma_M\rightarrow\infty$, a critical value of σ_A, σ_{Ac}, at which the bifurcation $S_s\rightarrow S_d$ occurs, goes to $1/\sqrt{2}$.

Figure 1(b) shows the phase diagrams in the σ_A-b plane for various values of σ_M. When $\sigma_A=0$ there is a transition $S_s\rightarrow S_d$ at a critical value of b, b_c, as b increases. The structure of the phase portraits persists up to some value of σ_A, σ_{Ar}, above which the reentrant transition occurs. At large b the system is in the S_s phase, as b decreases the system goes to the S_d phase, and as b decreases further the system

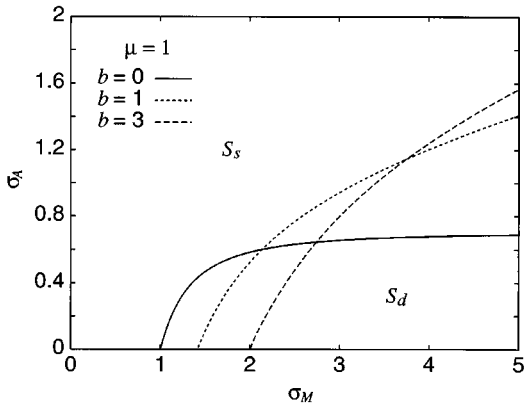

(a)

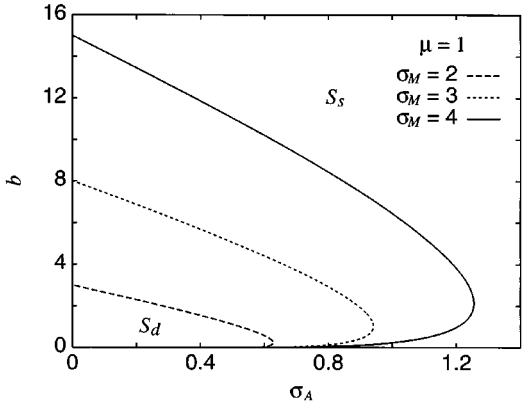

(b)

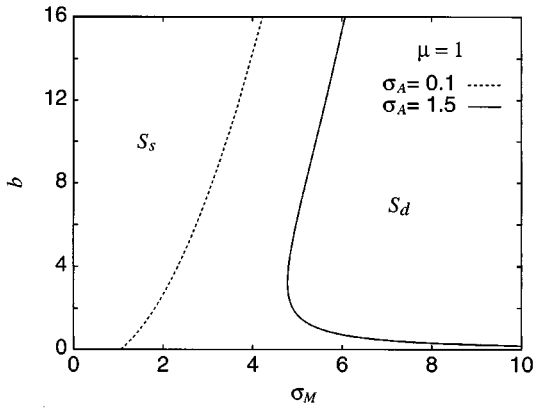

(c)

FIG. 1. Phase diagrams for $\mu=1$: (a) σ_M versus σ_A for various values of b, (b) σ_A versus b for various values of σ_M, and (c) σ_M versus b for various values of σ_A. S_s and S_d represent one-cluster and two-cluster phases, respectively.

reenters S_s phase. Because the pinning force ($b>0$) forces the system toward pinning at $\phi=0$ and depinning at $\phi=\pi$, it suppresses the multiplicative noise effect on the system. The additive noise also suppresses the effect of the pinning force as well as the multiplicative noise. Thus the effects of additive and mulitplicative noises and the pinning force frustrate the clustering tendency and lead to the reentrant transition. Figure 1(c) shows the phase diagrams in the

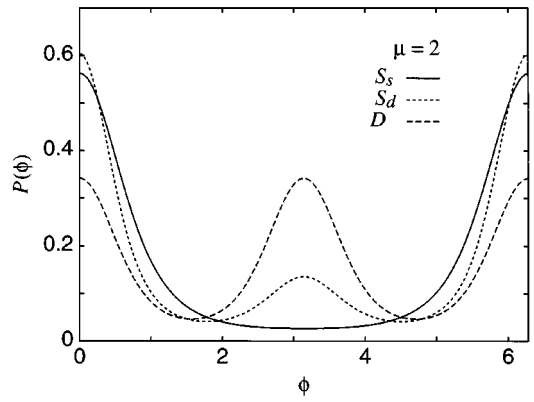

FIG. 2. Plot of $P(\phi)$ as a function of ϕ for $\mu=2$: solid line, $\sigma_M=0.5$, $\sigma_A=0.6$, and $b=0.2$ in the one-cluster (S_s) phase; dotted line, $\sigma_M=1$, $\sigma_A=0.7$, and $b=1.0$ in the two-cluster (S_d) phase; and dashed line, $b=2\sigma_A^2$ in the symmetric two-cluster (D) phase.

σ_M-b plane for various values of σ_A. For small σ_A, σ_{Mc} increases monotonically as b increases. For large σ_A there is a reentrant transition $S_s \rightarrow S_d \rightarrow S_s$ as b increases. This is also an illustration of the counteracting effects of additive versus multiplicative noise and the pinning force.

B. $\mu=2$

When $\mu=2$, performing the integration in Eq. (18) we obtain

$$P(\phi)=Z^{-1}(1+A\cos\phi)^{\beta/2-\gamma-(2-\nu)/2} \times(1-A\cos\phi)^{-\beta/2-\gamma-(2-\nu)/2}, \tag{32}$$

where

$$\beta=\frac{1}{\sigma_M\sqrt{\sigma_A^2+\sigma_M^2\Delta^2}},$$
$$\gamma=\frac{b}{\sigma_M^2\Delta^2}, \tag{33}$$
$$A=\frac{\sigma_M\Delta}{\sqrt{\sigma_A^2+\sigma_M^2\Delta^2}}$$

with the self-consistent equation (20). For given values of β, γ, and A, Δ can be obtained from Eq. (20) together with Eq. (32) and σ_A, σ_M, and b are related by

$$\sigma_M=\sqrt{\frac{A}{\beta\Delta(A,\beta,\gamma)}},$$
$$\sigma_A=\sqrt{\frac{(1-A^2)\Delta(A,\beta,\gamma)}{\beta A}}, \tag{34}$$
$$b=\frac{\gamma A\Delta(A,\beta,\gamma)}{\beta}.$$

When $b=0$, there is no symmetry-breaking transition because of the absence of the pinning force. As discussed in

Sec. III, for finite b, $P(\phi)$ shows the symmetry-breaking transition at a critical additive noise intensity $\sigma_{Ac}(b)$ given by Eq. (24). $\sigma_{Ac}(b)$ is independent of σ_M. In Fig. 4(b) we show the critical line that separates the symmetric (D) phase from the asymmetric (S_s and S_d) phases. For small σ_A, the system is in the asymmetric phases, and as σ_A increases, the transition to the symmetric phase occurs at $\sigma_{Ac}(b)$. As b goes to zero, $\sigma_{Ac}(b)$ approaches $1/\sqrt{2}$, and as b increases, $\sigma_{Ac}(b)$ also increases monotonically.

$P(\phi)$ has a maximum at $\phi=0$ or 2π and extrema at the roots of the equation

$$\sin\phi[(2\gamma+2-\nu)A\cos\phi+\beta]=0\,. \tag{35}$$

With a definition of $\Gamma\equiv\beta/(2\gamma+2-\nu)A$, Eq. (32) shows that for $\Gamma>1$, $P(\phi)$ has a minimum at $\phi=\pi$, and for $\Gamma<1$, $P(\phi)$ has a local maximum at $\phi=\pi$ and a minimum at $\phi=\cos^{-1}(-\Gamma)$. The critical point $\Gamma=1$ at which there is a bifurcation $S_s\rightarrow S_d$ is given by Eq. (34) with

$$\beta=(2\gamma+2-\nu)A \tag{36}$$

for $A\in[0,1]$ and $\gamma\in[0,\infty]$. Figure 2 shows $P(\phi)$'s in S_s, S_d, and D states.

For given b and σ_M the critical line (36) with Eq. (34) gives Δ in terms of b and σ_M as

$$\Delta=\frac{1\pm\sqrt{1-8(2-\nu)\sigma_M^2}}{2(2-\nu)\sigma_M^2}\equiv\Delta_{\pm}\,. \tag{37}$$

Since Δ is an average of $\cos\phi$ with a weight function $P(\phi)$, it has the restriction $|\Delta|<1$. This restriction with Eq. (37) divides the b-σ_M plane into three domains, in which satisfying Δ is given by

$$\Delta=\begin{cases}\Delta_{\pm} & \text{for } b<\dfrac{1}{4},\ \sqrt{\dfrac{1-2b}{2-\nu}}<\sigma_M<\sqrt{\dfrac{1}{8(2-\nu)b}}\\[2ex] \Delta_{-} & \text{for } b<\dfrac{1}{2},\ \sigma_M<\sqrt{\dfrac{1-2b}{2-\nu}}\\[2ex] 0 & \text{otherwise.}\end{cases} \tag{38}$$

In the domain with $\Delta=\Delta_{\pm}$, there are two transition points $\sigma_{An}^{(\pm)}$ at which the noise-induced transition occurs. This implies that there is a reentrant transition. In the domain with $\Delta=\Delta_{-}$, there is a single transition point σ_{An}. In the domain in which there is no satisfying Δ, the noise-induced transition does not occur as σ_A increases. The three domains are shown in Fig. 3 for $\nu=1$.

In the domains Eq. (38) with Eqs. (20), (32), (34), (36), and (37), we obtain the phase diagrams in the parameter space spanned by σ_A, σ_M, and b. Figure 4(a) shows the phase diagrams in the σ_A-σ_M plane for various values of b with $\nu=1$. In the limit $b\rightarrow 0$ [the solid line in Fig. 4(a)], for $\sigma_A=0$ the transition $S_s\rightarrow S_d$ occurs at $\sigma_M=\sigma_{Mc}\equiv 1$. For $\sigma_M<\sigma_{Mc}$, the system is on the S_s state, and for $\sigma_M>\sigma_{Mc}$, it is on the S_d state. This is a bifurcation induced by the multiplicative noise. As σ_A increases, the phase structure persists up to $\sigma_{Ac}\equiv 1/\sqrt{2}$, increasing σ_{Mc}, which implies that the additive noise suppresses the effect of the multiplicative noise in the system. At $\sigma_A=\sigma_{Ac}$, there is a symmetry-breaking transition for all values of σ_M leading to the D state.

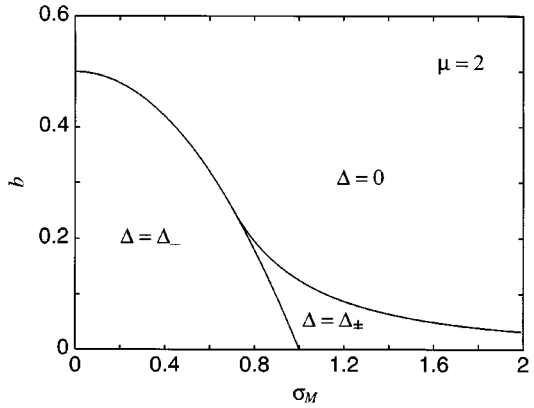

FIG. 3. Domains in the b-σ_M plane characterized by the solution of the self-consistent equation (domain): While the $\Delta=0$ domain represents no noise-induced transition, in the $\Delta=\Delta_{-}$ domain there is a noise-induced transition. In the $\Delta=\Delta_{\pm}$ domain there is a reentrant transition.

As b increases up to 1/4 [the dotted line in Fig. 4(a) for $b=0.1$], for small σ_A the phase structure persists, i.e., at $\sigma_A=0$ there is a transition $S_s\rightarrow S_d$ at $\sigma_{Mc}(b)<\sigma_{Mc}(b=0)$, and as σ_A increases up to some value σ_{A1}, $\sigma_{Mc}(b)$ increases. As σ_A increases above σ_{A1} up to σ_{A2}, $\sigma_{Mc}(b)$ decreases vanishing at $\sigma_{A2}<\sigma_{Ac}(b)$. This leads to the reentrant transition $S_d\rightarrow S_s\rightarrow S_d$ as σ_A increases for intermediate values of σ_M. This reentrant transition comes from the role of σ_A that restores the translational symmetry broken by the pinning force leading to the two-cluster state. For $\sigma_A>\sigma_{Ac}(b)$ given by Eq. (24), the system is on the D state regardless of the value of σ_M. As b increases further, the S_s phase reduces and vanishes at $b=1/2$. For $1/4<b<1/2$ [the dashed line in Fig. 4(a) for $b=0.3$], as σ_A increases σ_{Mc} decreases, vanishing at σ_{A2} without the reentrant transition. For $b>1/2$, there is no noise-induced transition except for the symmetry-breaking transition $S_d\rightarrow D$ at $\sigma_{Ac}(b)$. This comes from the pinning force, which tends to pin the system at two points $\phi=0$ and π.

Figure 4(b) shows the phase diagrams in the σ_A-b plane for various values of σ_M with $\nu=1$. When $\sigma_M=0$, Eq. (32) is reduced to

$$P(\phi)=Z^{-1}\exp\left[\frac{1}{\sigma_A^2}(\Delta\cos\phi+b\cos^2\phi)\right]\,. \tag{39}$$

With the self-consistent equation (20), the transition $S_s\rightarrow S_d$ occurs at the transition points

$$b=\frac{1}{2}\frac{\displaystyle\int_0^{2\pi}\cos\phi\exp[x(2\cos\phi+\cos^2\phi)]d\phi}{\displaystyle\int_0^{2\pi}\exp[x(2\cos\phi+\cos^2\phi)]d\phi}\,,$$
$$\sigma_A=\sqrt{\frac{b}{x}} \tag{40}$$

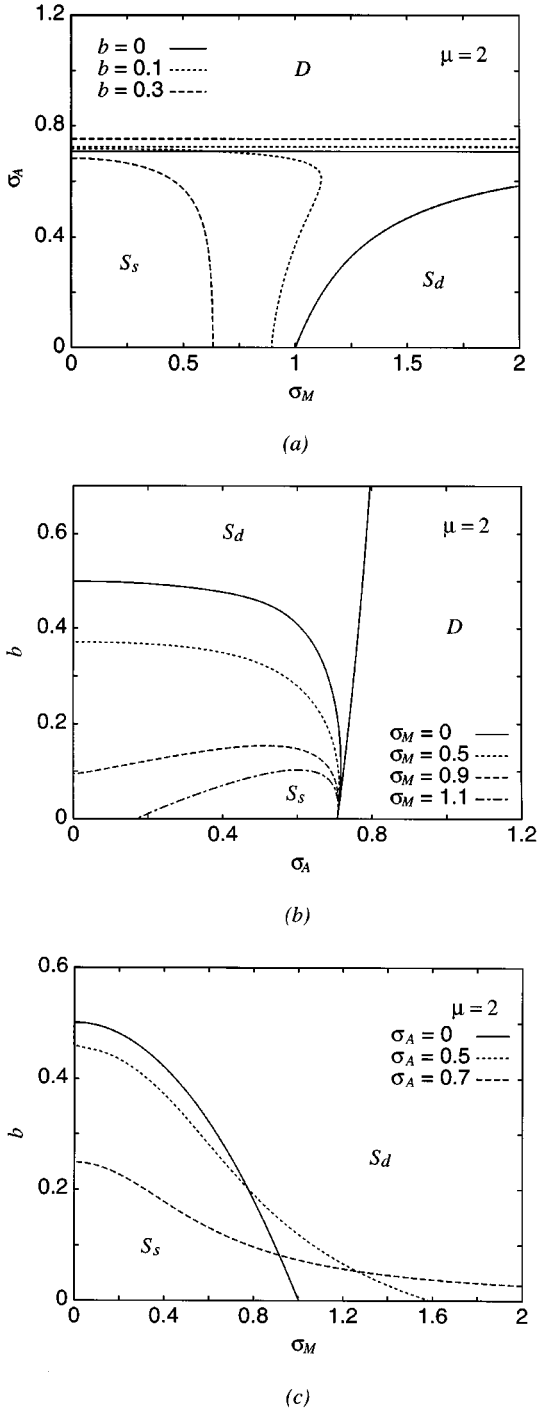

FIG. 4. Phase diagrams for $\mu=2$: (a) σ_M versus σ_A for various values of b, (b) σ_A versus b for various values of σ_M, and (c) σ_M versus b for various values of σ_A. S_s, S_d, and D represent one-cluster, two-cluster, and symmetric two-cluster phases, respectively.

for $x\in(0,\infty)$. The solid line in Fig. 4(b) represents the transition points. For small b there are two transition points σ_{A2} and σ_{Ac}, $\sigma_{A2}<\sigma_{Ac}$, at which the noise-induced transition $S_s\rightarrow S_d$ and the symmetry-breaking transition $S_d\rightarrow D$ occur, respectively. As b increases the phase structure persists up to $b_{c1}=1/5$, increasing σ_{Ac} and σ_{A2}. As b increases further up to $b=1/5$, σ_{A2} begins to decrease, leading to a small reentrant region in σ_A, and vanishes at $b=1/2$. For $b>1/2$, there is no S_s phase and only the symmetry-breaking transition $S_d\rightarrow D$ exists.

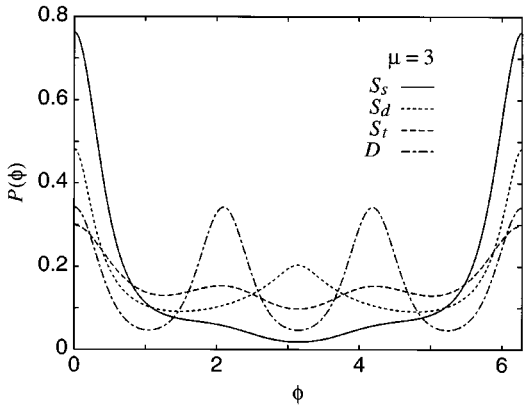

FIG. 5. Plot of $P(\phi)$ as a function of ϕ for $\mu=3$: solid line, $\sigma_M=1$, $\sigma_A=0.5$, and $b=0.4$ in the one-cluster (S_s) phase; dotted line, $\sigma_M=10$, $\sigma_A=0.5$, and $b=0.4$ in the two-cluster (S_d) phase; dashed line, $\sigma_M=3$, $\sigma_A=0.7$, and $b=0.4$ in the three-cluster (S_t) phase; and dot-dashed line, $b=3\sigma_A^2$ in the symmetric three-cluster (D) phase.

As σ_M increases, the phase structure persists up to $\sigma_M=1/\sqrt{2}$, reducing the S_s phase [the dotted line in Fig. 4(b) for $\sigma_M=0.5$]. For $1/\sqrt{2}<\sigma_M<1$ [the dashed line in Fig. 4(b) for $\sigma_M=0.9$], a reentrant transition $S_d\rightarrow S_s\rightarrow S_d$ occurs as σ_A increases for a given intermediate b. For $\sigma_A>\sigma_{Ac}(b)$, the system is on the D phase. For $\sigma_M>1$ [dot-dashed line in Fig. 4(b) for $\sigma_M=1.1$], in the limit $b\rightarrow 0$, there are two transition points at which the noise-induced transition $S_d\rightarrow S_s$ and the symmetry-breaking transition $S_s\rightarrow D$ occur as σ_A increases. As b increases, the reentrant transition occurs up to some value of b, above which there is no noise-induced transition except the symmetry breaking transition.

Figure 4(c) shows the phase diagrams in the σ_M-b plane for various values of σ_A with $\nu=1$. When $\sigma_A=0$ [solid line in Fig. 4(c)], for small b there is a critical value of σ_M, σ_{Mc}, at which the transition $S_s\rightarrow S_d$ occurs. For $\sigma_M<\sigma_{Mc}$, the system is on the S_s state, and for $\sigma_M>\sigma_{Mc}$, it is on the S_d state. The phase structure persists up to some value of b, $b_c=1/2$, decreasing σ_{Mc}. At $b=b_c$, σ_{Mc} vanishes, and above b_c, the system is on the S_d phase for all values of σ_M. As σ_A increases the phase structure persists up to $\sigma_{Ac}=1/\sqrt{2}$, decreasing b_c and increasing σ_{Mc} [see the dotted and dashed lines in Fig. 4(c) for $\sigma_A=0.5$ and 0.7, respectively]. At $\sigma_A=\sigma_{Ac}$, the symmetry-breaking transition occurs, leading to the D phase for $\sigma_A>\sigma_{Ac}$ for all values of σ_M and b.

C. $\mu=3$

When $\mu=3$, performing the integration in Eq. (18) we obtain

$$P(\phi)=Z^{-1}\exp[-\gamma\cos\phi](1+A\cos\phi)^{\beta-(2-\nu)/2}\times(1-A\cos\phi)^{-\beta-(2-\nu)/2}, \tag{41}$$

where

$$\beta=\frac{(\Delta+3b)\sigma_M^2\Delta^2+4b\sigma_A^2}{2\sigma_M^2\Delta^2\sqrt{\sigma_A^2+\sigma_M^2\Delta^2}},$$

$$\gamma=\frac{4b}{\sigma_M^2\Delta^2}, \tag{42}$$

$$A=\frac{\sigma_M\Delta}{\sqrt{\sigma_A^2+\sigma_M^2\Delta^2}},$$

with the self-consistent equation (20). For given values of β, γ, and A, Δ can be obtained from Eq. (20) together with Eq. (41) and σ_M, σ_A, and b are related by

$$\sigma_M=\sqrt{\frac{4A}{(8\beta A+\gamma A^2-4\gamma)\Delta(A,\beta,\gamma)}},$$

$$\sigma_A=\sqrt{\frac{4(1-A^2)\Delta(A,\beta,\gamma)}{A(8\beta A+\gamma A^2-4\gamma)}}, \tag{43}$$

$$b=\frac{A\gamma\Delta(A,\beta,\gamma)}{8\beta A+\gamma A^2-4\gamma}.$$

When $b=0$, there is no symmetry-breaking transition because of the absence of the pinning force. As discussed in Sec. III, for finite b, $P(\phi)$ shows the symmetry-breaking transition at a critical additive noise intensity $\sigma_{Ac}=1/\sqrt{2}$ independent of σ_M and b. In Fig. 7(b) we show the phase portrait that separates the symmetric (D) phase from the asymmetric (S) phase. For small σ_A, the system is in the asymmetric phase and as σ_A increases the transition to the symmetric phase occurs at σ_{Ac}.

$P(\phi)$ has a maximum at $\phi=0$ or 2π and extrema at the roots of the equation

$$\sin\phi(\cos\phi-\Gamma_+)(\cos\phi-\Gamma_-)=0, \tag{44}$$

with

$$\Gamma_\pm=\frac{-(2-\nu)A\pm\sqrt{(2-\nu)^2A^2+4\gamma(\gamma-2\beta A)}}{2\gamma A}. \tag{45}$$

When $|\Gamma_+|>1$, $P(\phi)$ has a peak at $\phi=0$ leading to the S_s phase, and when $|\Gamma_+|<1$ and $|\Gamma_-|>1$, $P(\phi)$ has two peaks at $\phi=0$ and π leading to the S_d phase. When $|\Gamma_-|<1$, $P(\phi)$ has three peaks at $\phi=0$, $\cos^{-1}(\Gamma_-)$, and $2\pi-\cos^{-1}(\Gamma_-)$ leading to the three-cluster (S_t) phase. Thus there are bifurcations $S_s\rightarrow S_d$ and $S_d\rightarrow S_t$ at the critical points $|\Gamma_+|=1$ and $|\Gamma_-|=1$, respectively. Figure 5 shows the $P(\phi)$'s in the S_s, S_d, S_t, and D phases.

Introducing X, Y, and Z defined by

$$X=\frac{\Delta}{b}, \quad Y=\frac{\sigma_M^2\Delta^2}{b}, \quad Z=\frac{\sigma_A^2}{4b}, \tag{46}$$

Eq. (44) is reduced to

$$\sin\phi\left[\left(\cos\phi+\frac{2-\nu}{8}Y\right)^2+\frac{X-1}{4}-\left(\frac{2-\nu}{8}Y\right)^2\right]=0, \tag{47}$$

leading to the following phase separations:

$$\begin{aligned}&S_t \text{ phase} \quad \text{for } (2-\nu)Y-3<X<\frac{(2-\nu)^2}{16}Y^2+1, \quad X,Y>0,\\ &S_d \text{ phase} \quad \text{for } 0<X<(2-\nu)Y-3,\\ &S_s \text{ phase} \quad \text{otherwise}.\end{aligned} \tag{48}$$

The phase separations are independent of Z. The phase portraits in the X-Y plane for $\nu=1$ are shown in Fig. 6.

With Eqs. (20), (41), (43), and (46) the phase separations (48) give the phase portraits in the parameter space spanned by σ_A, σ_M, and b. Figure 7(a) shows the phase diagrams in σ_A-σ_M plane for various values of b with $\nu=1$. When $b=0$ [solid line in Fig. 7(a)] the phase portrait is the same as that discussed in Sec. IV B. For small b [dotted line in Fig. 7(a) for $b=0.2$], when $\sigma_A=0$ there is a critical value of σ_M, σ_{Mc}, at which the transition $S_s\rightarrow S_d$ occurs as σ_M increases. This is a bifurcation induced by the multiplicative noise.

As σ_A increases, the phase structure persists up to some value of σ_A, σ_{A1}, increasing σ_{Mc}, which implies that the additive noise suppresses the effect of the multiplicative noise on the system. At $\sigma_A=\sigma_{A1}$ the S_t state appears and as σ_A increases above σ_{A1} there are two transition points σ_{Mc1} and σ_{Mc2} at which the transitions $S_s\rightarrow S_t$ and $S_t\rightarrow S_d$ occur, respectively. The existence of the S_t state results from the symmetry of the pinning force, which tends to pin the system at $\phi=0$, $2\pi/3$, and $4\pi/3$. As σ_A increases further the phase structure persists up to some value of σ_A, σ_{A2}, increasing σ_{Mc1} and σ_{Mc2} and expanding the S_t phase. As σ_A increases above σ_{A2}, σ_{Mc1} decreases and vanishes at σ_{A3}, shrinking the S_s phase. For a given intermediate σ_M, as σ_A increases the reentrant transition $S_d\rightarrow S_t\rightarrow S_s\rightarrow S_t$ occurs. This reentrant transition comes from the fact that the additive noise restores the symmetry broken by the pinning force. At $\sigma_A=\sigma_{Ac}$ the symmetry-breaking transition occurs leading to the D state above σ_{Ac} for all values of σ_M and b.

As b increases the phase structure persists up to some value of b, b_{c1}, increasing σ_{Mc} and σ_{Mc2} and decreasing σ_{Mc1}, σ_{A1}, and σ_{A2}, i.e., expanding the S_t phase and shrinking the S_s and the S_d phases. As b increases above b_{c1} [dashed line in Fig. 7(a) for $b=0.7$], when $\sigma_A=0$ there are two transition points σ_{Mc1} and σ_{Mc2} at which the transitions $S_s\rightarrow S_t$ and $S_t\rightarrow S_d$ occur, respectively. As σ_A increases the phase structure persists up to some value of σ_A, σ_{A3}, in-

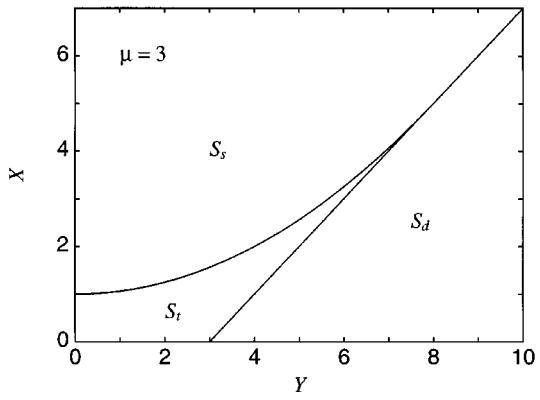

FIG. 6. Phase diagrams for $\mu=3$ in X-Y plane, where X and Y are defined by Eq. (46).

creasing σ_{Mc2} and decreasing σ_{Mc1}. At $\sigma_A=\sigma_{A3}$, σ_{Mc1} vanishes and above σ_{A3} there is no S_s phase. As b increases the phase structure persists up to some value of b, $b_{c2}=1$, shrinking the S_s phase and the S_d phase and expanding the S_t phase. For $b>b_{c2}$ [dot-dashed line in Fig. 7(a) for $b=1.1$], there is no S_s phase, and for small σ_A there is a transition point σ_{Mc} of $S_t\rightarrow S_d$ as σ_M increases. As σ_A increases σ_{Mc} also increases. When $\sigma_A=\sigma_{Ac}$, the symmetry-breaking transition occurs.

Figure 7(b) shows the phase diagrams in the σ_A-b plane for various values of σ_M with $\nu=1$. When $\sigma_M=0$, Eq. (41) is reduced to

$$P(\phi)=Z^{-1}\exp\left[\frac{1}{\sigma_A^2}\{\Delta\cos\phi+b\cos(3\phi)\}\right]. \qquad (49)$$

With the self-consistent equation (20), the transition $S_s\rightarrow S_t$ occurs at the transition points

$$b=\frac{\int_0^{2\pi}\cos\phi\exp[x\cos^3\phi]d\phi}{\int_0^{2\pi}\exp[x\cos^3\phi]d\phi}, \quad \sigma_A=\sqrt{\frac{4b}{3x}} \qquad (50)$$

for $x\in(0,\infty)$. The solid line in Fig. 7(b) represents the transition points. For small b there are two critical points σ_{An} and σ_{Ac}, $\sigma_{An}<\sigma_{Ac}$, at which the noise-induced transition $S_s\rightarrow S_t$ and the symmetry-breaking transition $S_t\rightarrow D$ occur, respectively. As b increases the phase structure persists decreasing σ_{An} and vanishing at $b=b_c=1$. For $b>b_c$, there is no S_s phase and only the symmetry-breaking transition $S_t\rightarrow D$ exists.

As σ_M increases, the phase structure persists up to some value of σ_M, $\sigma_{Mc}=1$, decreasing b_c [see the dotted line in Fig. 7(b) for $\sigma_M=1$]. When $\sigma_M>1$, the S_d phase appears for small b and σ_A. For small b, there are three transition points σ_{A1}, σ_{A2}, and σ_{Ac} at which the transitions $S_d\rightarrow S_s$, $S_s\rightarrow S_t$, and $S_t\rightarrow D$ occur, respectively. The phase structure persists up to some value of b, b_{c1}, decreasing σ_{A1} and σ_{A2}. As b increases above b_{c1}, four transition points σ_{A1}, σ_{A2}, σ_{A3}, and σ_{Ac} of $S_d\rightarrow S_t$, $S_t\rightarrow S_s$, $S_s\rightarrow S_t$, and $S_t\rightarrow D$ exist, leading to the reentrant transition. As b increases, the phase structure persists up to some value of b, b_{c2}, decreasing σ_{A1} and σ_{A3} and increasing σ_{A2}. At $b=b_{c2}$, σ_{A1} vanishes, shrinking the S_d phase, and at $b=b_{c3}$, σ_{A2} and σ_{A3} coincides shrinking the S_s phase. As b increases further, the system undergoes a single transition $S_t\rightarrow D$, the symmetry-breaking transition, at $\sigma_A=\sigma_{Ac}$. As σ_M increases further, b_{c2} increases and b_{c3} decreases, expanding the S_d phase and reducing the S_s phase.

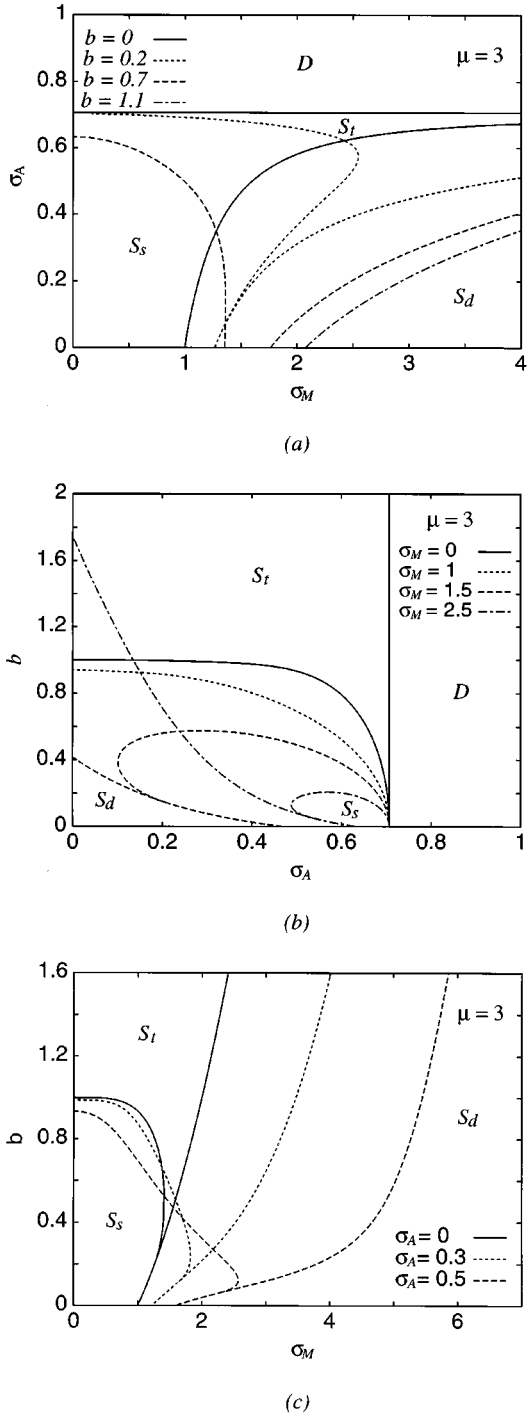

FIG. 7. Phase diagrams for $\mu=3$: (a) σ_M versus σ_A for various values of b, (b) σ_A versus b for various values of σ_M, and (c) σ_M versus b for various values of σ_A. S_s, S_d, S_t, and D represent one-cluster, two-cluster, three-cluster, and symmetric three-cluster phases, respectively.

Figure 7(c) shows the phase diagrams in the σ_M-b plane for various values of σ_A with $\nu=1$. When $\sigma_A=0$ [solid line in Fig. 7(c)], for $b=0$ there is a critical value of σ_M, $\sigma_{Mc}=1$, at which the transition $S_s \rightarrow S_d$ occurs. For $\sigma_M<\sigma_{Mc}$, the system is on the S_s state, and for $\sigma_M>\sigma_{Mc}$, it is on the S_d state. As b increases, the phase structure persists up to some critical value of b, b_{c1}, increasing σ_{Mc}. At $b=b_{c1}$, the S_t phase appears. As b increases above b_{c1} up to some value of b, $b_{c2}=1$, there are two transition points σ_{Mc1} and σ_{Mc2}, at which the transitions $S_s \rightarrow S_t$ and $S_t \rightarrow S_d$ occur, respectively. At $b=b_{c2}$, σ_{Mc1} vanishes, shrinking the S_s phase. For $b>b_{c2}$, only the transition $S_t \rightarrow S_d$ exists at σ_{Mc2}, which increases as b increases. As σ_A increases the phase structure persists up to $\sigma_{Ac}=1/\sqrt{2}$, increasing σ_{Mc}, σ_{Mc1}, and σ_{Mc2} and decreasing b_{c1} and b_{c2} [see the dotted and dashed lines in Fig. 7(c) for $\sigma_A=0.3$ and 0.5, respectively]. At $\sigma_A=\sigma_{Ac}$, the symmetry-breaking transition occurs, leading to the D phase for $\sigma_A>\sigma_{Ac}$ for all values of σ_M and b.

V. CONCLUSION

In this paper we have investigated the symmetry-breaking transition and the noise-induced transitions in coupled oscillator systems with the first, second, and third harmonic pinning forces subject to the fluctuating interaction with strength σ_M and the thermal additive noise with intensity σ_A. The system has a global inversion symmetry and global finite translation symmetry. While the inversion symmetry is not broken by the pinning force, the finite translation symmetry is broken by the pinning force. Since the additive noise restores the broken symmetry there is a critical intensity of the additive noise at which the symmetry-breaking transition occurs. The critical intensity of the additive noise does not depend on the intensity of the multiplicative noise, coupled to the phase differences of the oscillators. We have also obtained the critical exponent of the order parameter Δ.

In addition to the symmetry-breaking transition there are the noise-induced transitions due to the multiplicative noise characterized by the change of the number of peaks in the stationary probability distribution of the system. Each peak in the distribution has been identified as a cluster of like-phased oscillators. That is, we have interpreted the distribution as the instantaneous distribution of oscillator phases rather than as the distribution over time of the average phase. We found by the direct simulations of the globally coupled system that the cluster interpretation is valid.

In the system with the first harmonic pinning force, the multiplicative noise induces the noise-induced transition at the critical intensity of the multiplicative noise σ_{Mc}. For $\sigma_M<\sigma_{Mc}$ the system is in the one-cluster state and for $\sigma_M>\sigma_{Mc}$ it is in the two-cluster state. Since the first harmonic pinning force tends to pin the system at $\phi=0$ and to depin the system at $\phi=\pi$, it suppresses the effect of the multiplicative noise on the system. The additive noise also suppresses the effects of both the multiplicative noise and the pinning force, leading to the frustration among the additive and the multiplicative noises and the pinning force. The frustration induces the reentrant transitions in the σ_A-b and σ_M-b planes.

In the system with the second harmonic pinning force, since the pinning force tends to pin the system at $\phi=0$ and π, both the pinning force and the multiplicative noise induce the bifurcation from the one-cluster state to the two-cluster state. The additive noise suppresses both effects of the multiplicative noise and the pinning force and tends to restore the translation symmetry broken by the pinning force, leading to the symmetric two-cluster state. These conflicting roles of the additive noise lead to the reentrant transitions in the σ_M-σ_A and σ_A-b planes.

In the system with the third harmonic pinning force, since the pinning force tends to pin the system at $\phi=0$, $2\pi/3$, and $4\pi/3$, there exist three clustered phases, one-cluster, two-cluster, and three-cluster phases leading to the three kinds of noise-induced transitions between two of them. The conflicting roles of the additive and the multiplicative noises and the pinning force lead to the very rich structure of the phase portraits including the reentrant transition in the σ_A-σ_M, σ_A-b, and σ_M-b planes.

In conclusion, we have studied the phase transitions in the globally coupled oscillators with the additive and the multiplicative noises and the higher harmonic pinning force to understand the interplay of them. Their conflicting and frustrated roles have showed the very rich structure of phase portraits.

ACKNOWLEDGMENTS

This work was supported by the Ministry of Information and Communication, Korea. We are grateful to Dr. E. H. Lee for his support of this research. We appreciate discussions with Dr. C. R. Doering.

[1] W. Horsthemke and R. Lefever, *Noise-Induced Transitions* (Springer-Verlag, New York, 1984), and references therein.
[2] W. Horsthemke and M. Mansour, Z. Phys. B **24**, 307 (1976); W. Horsthemke and R. Lefever, Biophys. J. **35**, 415 (1981); W. Horthemke and R. Lefever, Phys. Lett. **A 64**, 19 (1977).
[3] F. Schloegel, Z. Phys. **253**, 147 (1972); S. Kabashima, S. Kogure, T. Kawakubo, and T. Okada, J. Appl. Phys. **50**, 6296 (1979).
[4] R. Graham, in *Phase-Transition-like Phenomena in Lasers and Nonlinear Optics*, edited by H. Haken (Teubner, Stuttgart, 1973).
[5] K. C. Shaing, Phys. Fluid **27**, 1924 (1984).
[6] A. Pacault and C. Vidal, *Synergetics. Far From Equilibrium* (Springer, New York, 1979); G. Nicolis, G. Dewel, and J. W. Turner, *Order and Fluctuations in Equilibrium and Nonequilibrium Statistical Mechanics* (Wiley, New York, 1981).
[7] C. Van den Broeck, J. M. R. Parrondo, J. Armero, and A. Hernández-Machado, Phys. Rev. E **49**, 2639 (1994); C. Van den Broeck, J. M. R. Parrondo, and R. Toral, Phys. Rev. Lett. **73**, 3395 (1994).
[8] A. Fulinski and T. Telejko, Phys. Lett. A **152**, 11 (1991).
[9] S. Kim and M. Y. Choi, Phys. Rev. B **48**, 322 (1993).

[10] Y. Kuramoto, *Chemical Oscillations, Waves, and Turbulence* (Springer, New York, 1984).
[11] D. Fisher, Phys. Rev. B **31**, 1396 (1985); S. H. Strogatz, C. M. Marcus, R. M. Westervelt, and R. E. Mirollo, Physica D **36**, 23 (1989).
[12] H. Sompolinsky, D. Golomb, and D. Kleinfeld, Phys. Rev. A **43**, 6990 (1991).
[13] S. H. Park and S. Kim, Phys. Rev. E **53**, 3425 (1996).
[14] S. Kim, S. H. Park, C. R. Doering, and C. S. Ryu, Phys. Lett. A (to be published); S. Kim, S. H. Park, and C. S. Ryu, ETRI J. **18**, 147 (1996).
[15] S. Shinomoto and Y. Kuramoto, Prog. Theor. Phys. **75**, 1105 (1986); C. Kurrer and K. Schulten, Physica D **50**, 311 (1991).
[16] H. Risken, *The Fokker-Planck Equation* (Springer-Verlag, New York, 1988).
[17] The Fokker-Planck equation in Ref. [13] was written for the Stratonovich interpretation. The authors were mistaken to state the Fokker-Planck equation as one for Itô interpretation. In the limit of zero additive noise the Fokker-Planck equation (11) agrees with the one of Ref. [13].